

Received:  
22 June 2015Revised:  
5 September 2016Accepted:  
12 September 2016<http://dx.doi.org/10.1259/bjr.20150502>

Cite this article as:

Roldan-Valadez E, Rios C, Motola-Kuba D, Matus-Santos J, Villa AR, Moreno-Jimenez S. Choline-to-*N*-acetyl aspartate and lipids-lactate-to-creatine ratios together with age assemble a significant Cox's proportional-hazards regression model for prediction of survival in high-grade gliomas. *Br J Radiol* 2016; **89**: 20150502.

## FULL PAPER

# Choline-to-*N*-acetyl aspartate and lipids-lactate-to-creatine ratios together with age assemble a significant Cox's proportional-hazards regression model for prediction of survival in high-grade gliomas

<sup>1</sup>ERNESTO ROLDAN-VALADEZ, MD, PhD, <sup>2</sup>CAMILO RIOS, PhD, <sup>3</sup>DANIEL MOTOLA-KUBA, MD, <sup>3</sup>JUAN MATUS-SANTOS, MD, <sup>4</sup>ANTONIO R VILLA, MD, MSc and <sup>5</sup>SERGIO MORENO-JIMENEZ, MD, PhD

<sup>1</sup>Direccion de Investigacion, Hospital General de México "Dr. Eduardo Liceaga", Mexico City, Mexico

<sup>2</sup>Department of Neurochemistry, National Institute of Neurology and Neurosurgery, Mexico City, Mexico

<sup>3</sup>Oncology Unit, Medica Sur Clinic and Foundation, Mexico City, Mexico

<sup>4</sup>Division de Investigacion, Facultad de Medicina, UNAM, Mexico City, Mexico

<sup>5</sup>Radioneurosurgery Unit, National Institute of Neurology and Neurosurgery, Mexico City, Mexico

Address correspondence to: Dr Ernesto Roldan-Valadez

E-mail: [ernest.roidan@usa.net](mailto:ernest.roidan@usa.net)

Ernesto Roldan-Valadez was Coordinator of Research at the MRI Unit of Medica Sur Clinic and Foundation from 2010 to April 2015.

**Objective:** A long-lasting concern has prevailed for the identification of predictive biomarkers for high-grade gliomas (HGGs) using MRI. However, a consensus of which imaging parameters assemble a significant survival model is still missing in the literature; we investigated the significant positive or negative contribution of several MR biomarkers in this tumour prognosis.

**Methods:** A retrospective cohort of supratentorial HGGs [11 glioblastoma multiforme (GBM) and 17 anaplastic astrocytomas] included 28 patients (9 females and 19 males, respectively, with a mean age of 50.4 years, standard deviation: 16.28 years; range: 13–85 years). Oedema and viable tumour measurements were acquired using regions of interest in  $T_1$  weighted,  $T_2$  weighted, fluid-attenuated inversion recovery, apparent diffusion coefficient (ADC) and MR spectroscopy (MRS). We calculated Kaplan-Meier curves and obtained Cox's proportional hazards.

**Results:** During the follow-up period (3–98 months), 17 deaths were recorded. The median survival time was 1.73 years (range, 0.287–8.947 years). Only 3 out of 20 covariates (choline-to-*N*-acetyl aspartate and lipids-lactate-to-creatine ratios and age) showed significance in explaining the variability in the survival hazards model; score test:  $\chi^2$  (3) = 9.098,  $p$  = 0.028.

**Conclusion:** MRS metabolites overcome volumetric parameters of peritumoral oedema and viable tumour, as well as tumour region ADC measurements. Specific MRS ratios (Cho/Naa, L-L/Cr) might be considered in a regular follow-up for these tumours.

**Advances in knowledge:** Cho/Naa ratio is the strongest survival predictor with a log-hazard function of 2.672 in GBM. Low levels of lipids-lactate/Cr ratio represent up to a 41.6% reduction in the risk of death in GBM.

## INTRODUCTION

Quantitative imaging methods have depicted potential parameters that are able to increase care and new developments in patient treatments.<sup>1</sup> In the case of brain tumours, there has been a long-lasting attention in the documentation of predictive biomarkers for gliomas,<sup>2</sup> supported by the fact that they constitute the most frequent primary brain tumours with a frequency of approximately

38%.<sup>3</sup> The majority of them are diagnosed with glioblastoma multiforme (GBM). Conventional imaging is considered the "tip of the iceberg" in current imaging of GBM, with a significant portion of the GBM cells already invading the peripheral tissue.<sup>4</sup> The biological behaviour of gliomas produces microscopic invasion in surrounding tissues, especially white matter (WM) tracts,<sup>5</sup> from the visible area of disease.<sup>6</sup> Then, normal appearance WM is a term used

when infiltration is not able to be detected using conventional imaging protocols of MR.<sup>7</sup> Nowadays, it is considered that regions of widespread oedema surrounding the tumour on  $T_2$  weighted imaging encompass neoplastic cells that have penetrated into WM regions.<sup>8</sup> These factors affect the survival rate of patients because after surgeons excise all radiologically visible portions of a tumour, the surgical margins may not be “clean”, and further neoplastic growth can occur in the adjacent brain, leading from microscopic residual to macroscopic recurrence.<sup>9</sup>

GBM shows a median survival of 14 months, which has not been increased by contemporary treatments.<sup>10</sup> The mean life expectancy in anaplastic astrocytoma (AA) is 41 months.<sup>11</sup> The biological behaviour of GBM and AA does not allow a total surgical resection without tumour recurrence. Integrative treatment approaches currently combine image-guided surgery supplemented by radiotherapy and chemotherapy.<sup>12</sup>

Predictive studies for survival in GBM have considered clinical factors such as the Karnofsky score, tumour location and size, histopathology, degree of resection, ionizing radiation, second surgery and genetics; however, many of these variables have shown conflicting results.<sup>2</sup> Some patients develop a satisfactory response, while others have an unsuccessful evolution.<sup>13</sup> Conventional MR examinations for the diagnosis of gliomas around the world are usually limited to identifying oedema boundaries and local tumour infiltration to those patterns detected in the  $T_1$  and  $T_2$  weighted images.<sup>14,15</sup> The apparent diffusion coefficient (ADC) has been proved to convey predictive value.<sup>16</sup> Similar results were found in the ratio of choline-to-*N*-acetyl aspartate (Cho/Naa) using MR spectroscopy (MRS)<sup>17</sup> and in the presence of immediate (<1 cm) and distant oedema (>1 cm), in the survival analysis of patients with GBM.<sup>15</sup>

Despite the growing evidence of studies exploring the prognostic ability of MR biomarkers in patients with high-grade gliomas (HGGs), a consensus of the best survival biomarkers is still missing in the literature. We considered it necessary to investigate additional evidence of potential quantitative MR biomarker contribution towards a positive or adverse effect on survival in these groups of patients. We aimed to assess the role of the fundamental demographics of a small group of patients together with conventional MR volumetric measurements, diffusion-weighted imaging (DWI) and MRS to detect which imaging variables are reliable parameters of overall survival (OS) in patients with AA and GBM.

## METHODS AND MATERIALS

### Patients

This retrospective study received approval from the local institutional review board. A retrospective cohort of 28 patients with AA and GBM underwent follow-up from December 1999 to January 2012. The cohort included 19 males and 9 females, with an average age of 50.4 years (standard deviation: 16.28; range: 13–85 years). We obtained patient post-operative survival times (in years) from the Oncology Unit tumour register database. Pathologic findings included 11 GBM and 17 anaplastic gliomas. We excluded cases with missing imaging data, structural abnormalities, histopathology or presence of artefacts and

also those with a previous history of surgery, ionizing radiation or chemotherapy. Most of the subjects received (after resection) the Stupp protocol. The histopathologic report followed the World Health Organization criteria.

### Brain image and data acquisition

Brain examination used a 3.0-T scanner (Signa HDxt; GE Healthcare, Waukesha, WI) with an eight-channel head coil (Invivo Corporation, Gainesville, FL). MR sequences included conventional  $T_2$  weighted imaging, fluid-attenuated inversion recovery (FLAIR), Spoiled Gradient Echo (SPGR), DWI and axial  $T_1$  weighted imaging, and contrast dose (Magnevist®; Schering, Berlin, Germany). DWI used  $b$ -values 0 and 1000 s $mm^{-2}$ . Figure 1 shows the appearance of conventional MRI sequences in a patient with GBM.

Axial MRS used the multivoxel Point resolved spectroscopy (PRESS) technique. The volume of interest size was positioned over the lesion, minimizing the effect of partial volume owing to neighbouring tissues including bones and cerebral spinal fluid of the ventricles. MRS was recorded with  $T_1$  weighted post-contrast images, field of view 24 × 24 cm, a 256 × 256 matrix size (frequency encoding steps) repetition time 1500 ms, echo time 26 and 144 ms, 1-cm section thickness and 24 × 24 phase encoding.

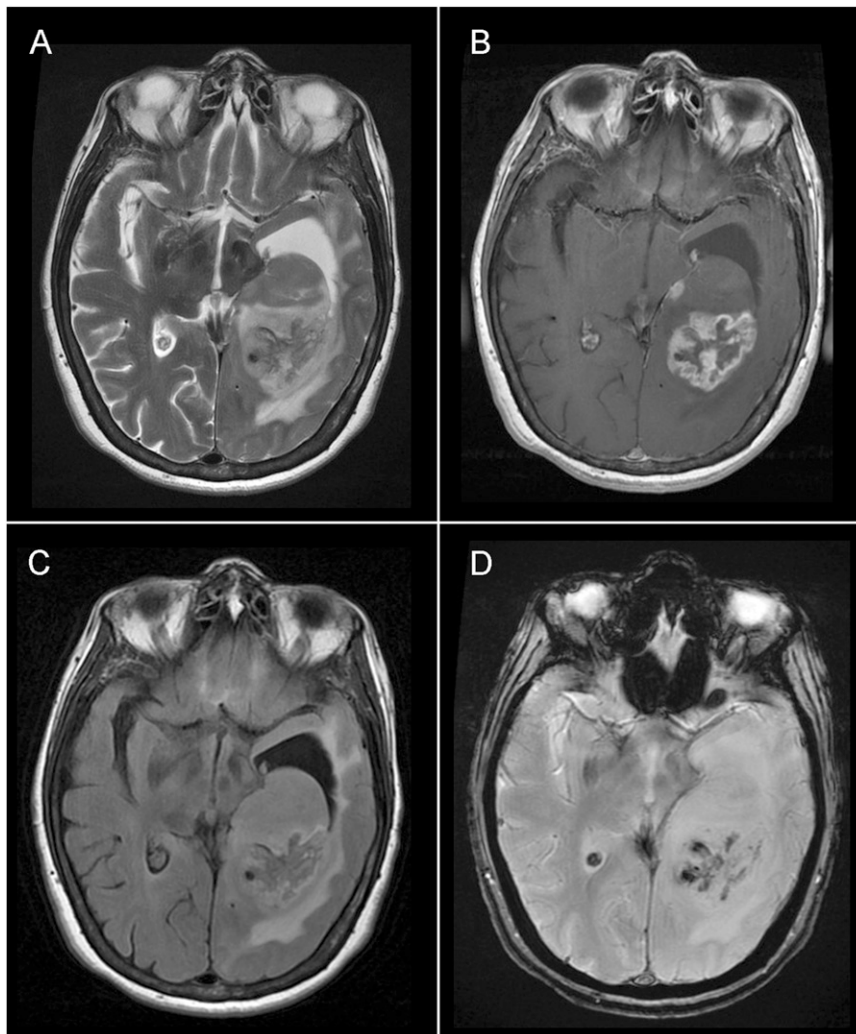
### Image post-processing and data analysis

One radiologist, blind to the clinical history of each patient, manually traced the boundaries of the tumour regions. We accepted  $T_1$  and  $T_2$  weighted images as the selected MRI sequences to evaluate the tumour size and extension of oedema, respectively.<sup>14</sup> In addition, we calculated volumes of the oedema and tumour regions to obtain objective measurements of the maximum extent of these tumour regions that we included in our statistic analysis:  $T_1$  weighted post-contrast volume,  $T_2$  weighted pre-contrast volume,  $T_1$  weighted/ $T_2$  weighted ratio, FLAIR pre-contrast volume and FLAIR to  $T_1$  weighted ratio. Additional  $T_1$  weighted to  $T_2$  weighted and FLAIR to  $T_1$  weighted ratio sequences intended to capture the relationship of oedema to tumour size in case any of these rates showed statistical significance as survival predictors.

We measured ADC at five tumour regions. The viable tumour region was the enhanced rim at  $T_1$  weighted post-contrast imaging, necrosis (the cystic cavity). We recorded two oedema regions: an immediate zone (a 1-cm-wide band) and distant zones (adjacent to the immediate area, also a 1-cm-wide band). In addition, a region of normal appearance WM was drawn in the patient contralateral hemisphere.

Metabolite signal peaks were analyzed from MRS and centred within a range of 0–4.35 ppm. They included *N*-acetyl aspartate (Naa) at 2.0 ppm, choline located at 3.2 ppm (Cho) and creatine (Cr) at 3–3.1 ppm. A compound peak containing lipids and lactate (LL) was found at 0.8–1.4 ppm, and two peaks of myo-Inositol were located at 3.56 and 4.06 ppm.<sup>18</sup> Automatic shimming and water suppression pulses were applied. Quantitative data were analyzed with the software FuncTool v. 9.4.04b (GE Medical Systems, Milwaukee, WI).

Figure 1. Conventional MRI sequences in a patient with glioblastoma multiforme: axial plane images in (a)  $T_2$  weighted, (b) post-gadolinium  $T_1$  weighted, (c) fluid-attenuated inversion recovery and (d) gradient echo.



### Survival time

Evolution of GBM monitored changes in baseline images acquired at the time of the first operation. OS counted time from the baseline to death or, in living patients, from the first MRI to last follow-up.

### Statistical analysis

According to the aims of the study, only 20 variables related to basic demographics and MRI biomarkers were included in the assessments. We recorded three variables related to clinical findings (gender, age, tumour grade). From the visual inspection of conventional MRI, we obtained two variables (affected side and tumour location). From the MRI sequences, five variables were calculated from the post-processing of volumetric measurements ( $T_1$  weighted post-contrast volume,  $T_2$  weighted pre-contrast volume,  $T_1$  weighted/ $T_2$  weighted ratio, FLAIR pre-contrast volume and FLAIR/ $T_1$  weighted ratio). The could measure ADC values at ROIs corresponding to five tumour regions (viable tumour region, necrosis, an immediate zone of oedema, a distant zone of oedema, normal-appearing WM). Finally, we only included five metabolites ratios, derived from

MRS metabolites quantification (Naa/Cr, Cho/Cr, LL/Cr, Cho/Naa and myo-Inositol/Cr). We used the Kaplan–Meier<sup>19</sup> and Cox’s proportional hazards model analyses.<sup>20</sup> For all analyses, statistical significance was accepted at  $p$ -value <5%. We used IBM SPSS® software v. 23.0.0.1 (IBM Corp., New York, NY; formerly SPSS Inc., Chicago, IL).

## RESULTS

### General data

Patients had a follow-up from 3 to 98 months with 17 deaths recorded. The median survival was 1.73 years (range, 0.287–8.947 years). Table 1 summarizes descriptive statistics of the selected variables; the survival curve for this cohort is depicted in Figure 2.

### Survival analysis

We performed consecutive Cox’s proportional hazards regression analyses, a first one to fit a null model containing only an intercept parameter (residual  $\chi^2(13) = 22.647$ ,  $p = 0.046$ ), which allowed us to select the major parameters of survival; in the first analysis, only the 3 variables with the smallest  $p$ -value (out of the 20 available covariates) were selected:

Table 1. Descriptive statistics of the selected variables

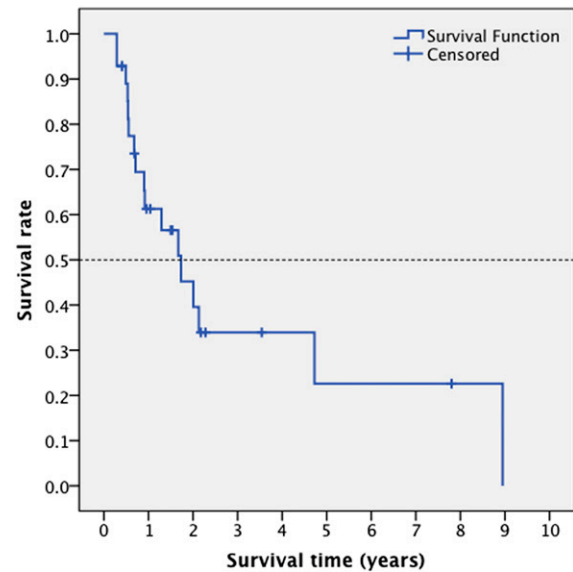
Categorical variables	Number	Percent
Gender		
Male	19	67.9%
Female	9	32.1%
Tumour grade		
III	11	39.3%
IV	17	60.7%
Cerebral hemisphere		
Left	13	52%
Right	8	32%
Both	4	16%
Tumour location		
Zone I	10	35.7%
Zone II	3	10.7%
Zone III	12	42.9%
Zone IV	3	10.7%
<i>Continuous variables</i>		
	<i>Mean</i>	<i>SD</i>
Age (years)	50.54	16.283
ADC tumour (mm <sup>2</sup> s <sup>-1</sup> )	0.001310	0.000391
ADC necrosis (mm <sup>2</sup> s <sup>-1</sup> )	0.002290	0.000927
ADC proximal oedema (mm <sup>2</sup> s <sup>-1</sup> )	0.001294	0.000460
ADC distal oedema (mm <sup>2</sup> s <sup>-1</sup> )	0.001323	0.000283
ADC normal tissue (mm <sup>2</sup> s <sup>-1</sup> )	0.000885	0.000200
Naa/Cr	0.874	0.637
Cho/Cr	2.353	1.190
Lipids–lactate/Cr	3.806	3.204
mI/Cr	1.572	1.272
Cho/Naa	3.613	2.033
Post-contrast T <sub>1</sub> volume (cm <sup>3</sup> )	24.047	29.551
Pre-contrast T <sub>2</sub> volume (cm <sup>3</sup> )	74.948	46.699
T <sub>1</sub> /T <sub>2</sub> volume ratio	0.337	0.316
FLAIR volume (cm <sup>3</sup> )	79.031	44.647
T <sub>1</sub> /FLAIR volume ratio	0.298	0.270

ADC, apparent diffusion coefficient; FLAIR, fluid-attenuated inversion recovery; mI, myo-Inositol; SD, standard deviation.

Cho/Naa ratio ( $p = 0.017$ ), age ( $p = 0.072$ ) and lipids–lactate/creatinine ( $p = 0.109$ ).

A second Cox's regression analysis used the three selected covariates. A regression analysis for age (years) and Cho/Naa and lipids–lactate/creatinine ratios provided an "Omnibus Test of Model Coefficients" that explained the survival hazards:  $\chi^2(3) = 9.098$ ,  $p = 0.028$ . For this new model, the  $-2 \times \log$  likelihood depicted an increased significance after adding the selected

Figure 2. A survival curve depicting the median survival time in patients with anaplastic astrocytoma and glioblastoma multiforme.



covariates:  $\chi^2(3) = 14.591$ ,  $p = 0.002$ . At the 0.05 level, the three covariates significantly affected the hazard function (Table 2).

Cho/Naa ratio was the strongest survival predictor with a log-hazard function of 2.672. This value indicated that for every additional unit increase in the Cho/Naa ratio, patients increased 2.672 times the hazard function to report a death stage compared to those who did not have an increase, controlling for all other factors in the model. The LL/Cr ratio depicted a log-hazard function of 0.584; considering the negative sign of its beta value, this hazard value can be interpreted as a 41.6% reduction in the risk to report a death stage. The age has a positive value with a log-hazard function of 1.062, indicating a 6.2% increase in the risk to report death for every additional year of the patient age. Figure 3a shows an axial plane of a FLAIR sequence depicting an HGG; a white arrow on the grid for multivoxel MRS points to an area of the solid tumour. Figure 3b shows the spectroscopy of the selected tumour region; the major increase of the Cho and LL peaks of the spectrum is evident, depicted by black arrows.

We completed our Cox's analysis by plotting the Schoenfeld residuals to check for proportional hazards;<sup>21</sup> they evaluated uncensored survival times. For the first two covariates (Cho/Naa and LL/Cr), the locally weighted scatterplot smoother (Lowess) curve varied in a non-systematic way from the zero reference line (Figure 4a,b). After the fourth year, we noticed a smooth line suggesting a trend over time with a negative slope; for both variables, the plots were based on only few events. Residuals showed a large influence on plots at the first-time points. For the covariate age, after the fourth year, the fitted line signals that the hazard ratio for this covariate increases over time (suggestive positive slope) (Figure 4c).

## DISCUSSION

Survival time for GBM continues to be approximately 1 year despite advances in surgery and treatment.<sup>2</sup> The presence of AA

Table 2. Wald's tests assessment of the covariates effects on the hazard function

Selected brain metabolites ratios	B	SE	$\chi^2$ (Wald test)	p-value	Log-hazard functions	95.0% CI	
						Lower	Upper
Cho/Naa ratio	0.983	0.448	4.821	0.028	2.672	1.111	6.423
LL/Cr ratio	-0.538	0.268	4.039	0.044	0.584	0.345	0.987
Age (years)	0.060	0.034	3.059	0.080	1.062	0.993	1.136

B, B values correspond to the standardized coefficient values in a constructed regression equation; CI, confidence interval; SE, standard error.

and GBM explains the median survival time of 1.73 years. Although some researchers reported a 3-year life period for patients with glioblastoma of 3% and a 5-year lifetime of 0%, there are citations of patients surviving GBM up to 10 years.<sup>22,23</sup>

To date, the usually selected variables for survival prediction in AA and GBM include age, Karnofsky score, tumour region and size, histopathology, the amount of resected tissue, ionizing radiation and additional surgeries. Although current studies combine clinical and genetics feature, there is still an exclusion of an integrative assessment of MR quantitative biomarkers (such as those from spectroscopy) in the prognosis.<sup>24</sup>

A biomarker is "a biologic feature measured and evaluated in an objective manner and considered an indicator of normal biologic processes, pathogenic processes or pharmacologic responses to a therapeutic intervention".<sup>25</sup> One of the most clinically relevant findings in our study was the evidence that the Cho/Naa ratio is a biomarker with a higher impact on the survival time ( $p < 0.028$ ). Recent studies proved that anti-angiogenic drugs can change the relation of the Cho to Naa ratio and as a consequence be predictors of treatment response.<sup>26</sup> Our data support a similar study using the same

index almost a decade ago, although that study did not report on the influence of lipids-lactate-to-creatine ratio;<sup>17</sup> a previous report found that MRS parameters may precede the perfusion abnormalities and contrast enhancement features in AA and GBM.<sup>27</sup> It is interesting for our group that despite the evidence supporting the use of these MR biomarkers, there is still not an international consensus whether the quantification of MRS metabolites becomes a supplement of the conventional MRI for brain tumours performed at most tertiary-care hospitals. The reality is that spectroscopy, MRI perfusion and quantitative DTI are not used to forestall brain tumour development on a day-to-day basis;<sup>12</sup> then, classic  $T_1$  weighted and  $T_2$  weighted features prevail as the diagnostic hallmarks.<sup>28</sup>

Recent studies have proved a significant association of ADC in subgroup stratification;<sup>16</sup> for example, in the degree of methylation by the O6-methylguanine-DNA methyltransferase (MGMT) promoter in patients with GBM.<sup>24</sup> However, these studies missed to complement their analyses including a Cox's regression model; simultaneous assessment of ADC values from several tumour regions did not provide significant biomarkers using a Cox's regression method.

Figure 3. (a) An axial plane of a fluid-attenuated inversion-recovery sequence is illustrating a high-grade glioma; a selected voxel on the grid MR spectroscopy (MRS) is pointing an area of solid tumour (white arrow). (b) In the MRS spectrum of a tumour region, the major increase of the Cho and LL peaks (black arrows) is evident.

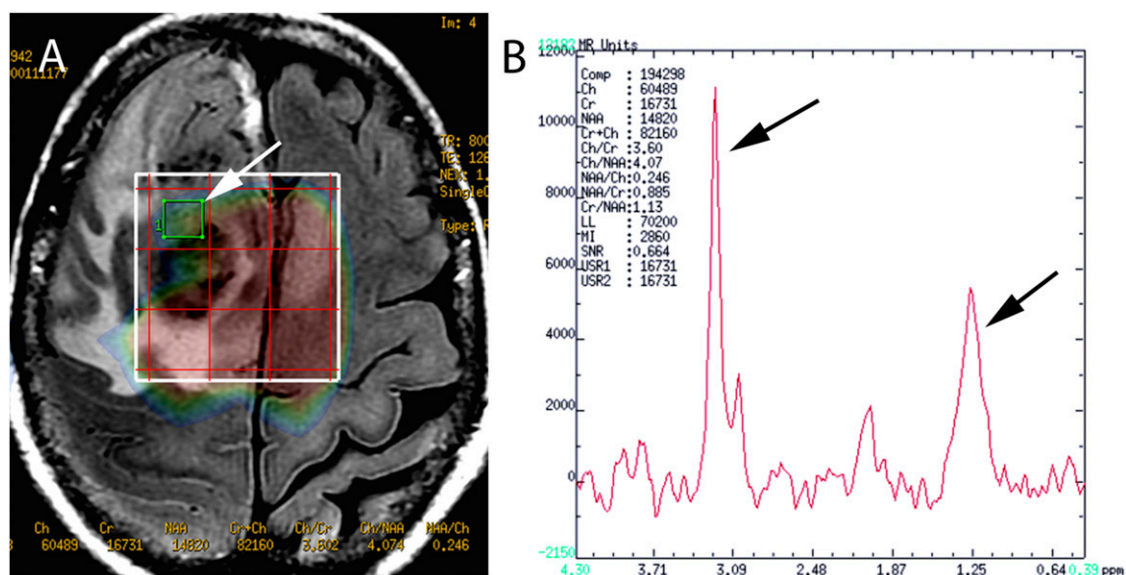
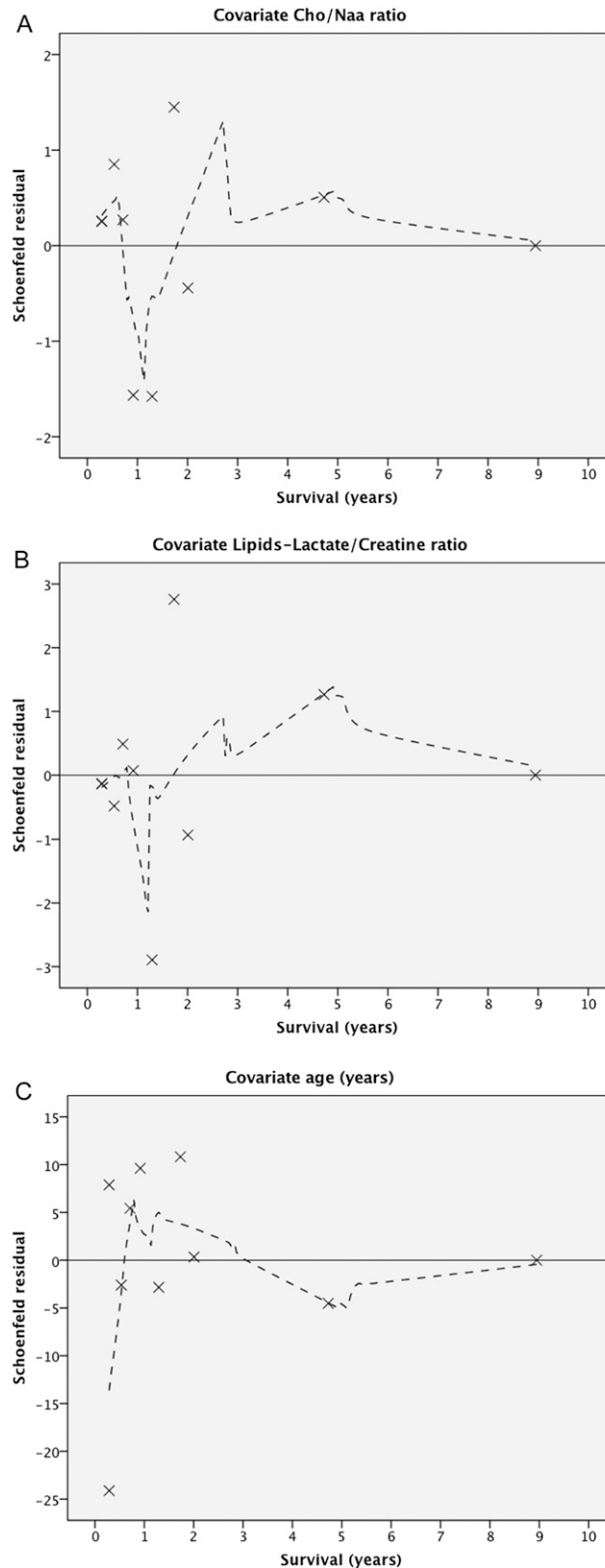


Figure 4. A residuals plot is depicting the selected variables in the survival model: (a) Cho/Naa ratio and (b) lipids-lactate/creatinine ratio; in both plots, the variation is noticeable in a non-systematic way, from the zero reference line, of the Lowess curves. After the fourth year, the smooth line reveals a tendency with a negative slope; for both variables, the plots represent few events, and the residuals were biased at the initial points. For the covariate age, after the fourth year, the fitted line shows a positive incline, signifying and increased hazard ratio (c).



The association between low levels of lactate and hypoxia in tumour tissue was reported four decades ago;<sup>29</sup> this evidence is relevant because under hypoxic conditions, the hypoxia-inducible factor upregulates the production of vascular endothelial growth factor (VEGF), which plays a part in the intrusion of neoplastic cells and angiogenesis.<sup>30</sup> In patients with HGGs, higher lipid and lactate levels measured by MRS associated with significantly worse OS have been observed.<sup>31</sup> Then, our finding that low levels of lipids–lactate/Cr ratio represent up to a 41.6% reduction in the risk of death is a reverse statement that augmented hypoxia within neoplastic cells is coupled with worse clinical results.<sup>32</sup>

A significant predictor of clinical response is the time of life at diagnosis.<sup>33</sup> Younger patients depict a longer survival time.<sup>34</sup> Our findings support the notion that increasing age shows a decreasing OS; we found an incremental hazard of death per year of age of 6%.

Although gender was not significant, we found a male dominance (67.8%), which is in agreement with most of the studies about incidence of malignant glial tumours in the literature.<sup>35</sup>

The assessment of quantitative MRI biomarkers is becoming standard in patients with tumour, but a real understanding of the significant effects of the several MR modalities is still in its early days. Several studies have reported that tumour regions influence OS;<sup>35,36</sup> other multivariate analyses found that the location of the tumour might have a better prognosis, but its effect size is not enough to define this feature as an independent factor.<sup>2,37</sup> In our analysis, we did not find a significant association between tumour region and survival.

We evaluated the effect of peritumoral oedema through measurements of three-dimensional volumes in  $T_2$  weighted and FLAIR sequences; although there is a significant association between larger volumes and smaller survival times,<sup>37</sup> no significant influence was found in our data set.

We acknowledge some limitations in this study: the data came from a retrospective cohort. Although the study answers the questions posed in the introduction (which MRI biomarkers have a significant association with the survival in patients with AA and GBM), several clinical and surgical variables were

intentionally out of the scope of this study: the extent of resection, radiation dose and adjuvant chemotherapy. We wanted to focus our research on the assessment of potential quantitative MR biomarkers without the influence of other clinical/surgical/radiotherapy variables. Metabolic changes in the phospholipid cell membrane turnover are associated with several metabolites such as glycerophosphocholine, phosphocholine and phosphoethanolamine, each one playing significant roles as indicators of tumour growth. The discrimination of these metabolites, however, cannot be performed using the conventional (1) Quantitative proton magnetic resonance spectroscopy (HMRS); it requires specialized hardware with (31) Quantitative phosphorus magnetic resonance spectroscopy (PMRS).<sup>38</sup> Then, the research on MR biomarkers still needs additional studies with prospective cohorts to conclude reliability of the selected variables and to promote generalizability of the results.

In conclusion, a higher pre-operative Cho-to-Naa ratio, a lower lipids–lactate-to-creatine ratio and years of age are significant predictors of survival that overcome the classic  $T_2$  weighted pre-gadolinium and  $T_1$  weighted post-gadolinium volumetric standards (representatives of peritumoral oedema and viable tumour, respectively) and the ADC measurements (diffusibility of water). We acknowledge that MRS can detect the conversion of normal tissue to tumour infiltration before conventional MR sequences show striking findings. Because MRS acquisition does not require contrast, MRI units around the world might adapt the post-processing methods of MRS to their contexts to validate data about diagnosis and treatment response. The availability of complex variables that a radiologist has to evaluate in an advanced brain MRI together with the use of multivariate assessment (Kaplan–Meir and Cox's regression analysis) represents an integrative approach (qualitative and quantitative) in the clinical evaluation of these patients.

## ACKNOWLEDGMENTS

The authors thank Dr Sebastian Castillo-Rodriguez, Department of Radiology at Medica Sur Clinic and Foundation, for his imaging post-processing support.

## FUNDING

The Medica Sur Clinic and Foundation partially supported this article.

## REFERENCES

- Buckler AJ, Bresolin L, Dunnick NR, Sullivan DC, Aerts HJ, Bendriem B, et al. Quantitative imaging test approval and biomarker qualification: interrelated but distinct activities. *Radiology* 2011; **259**: 875–84. doi: <http://dx.doi.org/10.1148/radiol.10100800>
- Tugcu B, Postalci LS, Gunaldi O, Tanriverdi O, Akdemir H. Efficacy of clinical prognostic factors on survival in patients with glioblastoma. *Turk Neurosurg* 2010; **20**: 117–25. doi: <http://dx.doi.org/10.5137/1019-5149.JTN.2461-09.4>
- Kleihues P, Louis DN, Scheithauer BW, Rorke LB, Reifenberger G, Burger PC, et al. The WHO classification of tumors of the nervous system. *J Neuropathol Exp Neurol* 2002; **61**: 215–25; discussion 226–9. doi: <http://dx.doi.org/10.1093/jnen/61.3.215>
- Wang CH, Rockhill JK, Mrugala M, Peacock DL, Lai A, Jusenius K, et al. Prognostic significance of growth kinetics in newly diagnosed glioblastomas revealed by combining serial imaging with a novel biomathematical model. *Cancer Res* 2009; **69**: 9133–40. doi: <http://dx.doi.org/10.1158/0008-5472.CAN-08-3863>
- Johnson PC, Hunt SJ, Drayer BP. Human cerebral gliomas: correlation of postmortem MR imaging and neuropathologic findings. *Radiology* 1989; **170**(Pt 1): 211–17. doi:

- <http://dx.doi.org/10.1148/radiology.170.1.2535765>
6. DeAngelis LM. Brain tumors. *N Engl J Med* 2001; **344**: 114–23. doi: <http://dx.doi.org/10.1056/NEJM200101113440207>
  7. Watanabe M, Tanaka R, Takeda N. Magnetic resonance imaging and histopathology of cerebral gliomas. *Neuroradiology* 1992; **34**: 463–9. doi: <http://dx.doi.org/10.1007/BF00598951>
  8. Kelly PJ, Daumas-Duport C, Kispert DB, Kall BA, Scheithauer BW, Illig JJ. Imaging-based stereotaxic serial biopsies in untreated intracranial glial neoplasms. *J Neurosurg* 1987; **66**: 865–74. doi: <http://dx.doi.org/10.3171/jns.1987.66.6.0865>
  9. Zimmerman RA. Imaging of adult central nervous system primary malignant gliomas. Staging and follow-up. *Cancer* 1991; **67**(Suppl. 4): 1278–83. doi: [http://dx.doi.org/10.1002/1097-0142\(19910215\)67:4+<1278::AID-CNCR2820671526>3.0.CO;2-U](http://dx.doi.org/10.1002/1097-0142(19910215)67:4+<1278::AID-CNCR2820671526>3.0.CO;2-U)
  10. Yaneva MP, Semerdjieva ML, Radev LR, Vlaikova MI. Postoperative chemoradiotherapy with temodal in patients with glioblastoma multiforme—survival rates and prognostic factors. *Folia Med (Plovdiv)* 2010; **52**: 26–33.
  11. Keles GE, Chang EF, Lamborn KR, Tihan T, Chang CJ, Chang SM, et al. Volumetric extent of resection and residual contrast enhancement on initial surgery as predictors of outcome in adult patients with hemispheric anaplastic astrocytoma. *J Neurosurg* 2006; **105**: 34–40. doi: <http://dx.doi.org/10.3171/jns.2006.105.1.34>
  12. Kuhnt D, Becker A, Ganslandt O, Bauer M, Buchfelder M, Nimsky C. Correlation of the extent of tumor volume resection and patient survival in surgery of glioblastoma multiforme with high-field intraoperative MRI guidance. *Neuro Oncol* 2011; **13**: 1339–48. doi: <http://dx.doi.org/10.1093/neuonc/nor133>
  13. Ron IG, Gal O, Vishne TH, Kovner F. Long-term follow-up in managing anaplastic astrocytoma by multimodality approach with surgery followed by postoperative radiotherapy and PCV-chemotherapy: phase II trial. *Am J Clin Oncol* 2002; **25**: 296–302. doi: <http://dx.doi.org/10.1097/00000421-200206000-00020>
  14. Seidel C, Dorner N, Osswald M, Wick A, Platten M, Bendszus M, et al. Does age matter?—A MRI study on peritumoral edema in newly diagnosed primary glioblastoma. *BMC Cancer* 2011; **11**: 127. doi: <http://dx.doi.org/10.1186/1471-2407-11-127>
  15. Schoenegger K, Oberndorfer S, Wuschitz B, Struhel W, Hainfellner J, Prayer D, et al. Peritumoral edema on MRI at initial diagnosis: an independent prognostic factor for glioblastoma? *Eur J Neurol* 2009; **16**: 874–8. doi: <http://dx.doi.org/10.1111/j.1468-1331.2009.02613.x>
  16. Ellingson BM, Cloughesy TF, Lai A, Mischel PS, Nghiemphu PL, Lalezari S, et al. Graded functional diffusion map-defined characteristics of apparent diffusion coefficients predict overall survival in recurrent glioblastoma treated with bevacizumab. *Neuro Oncol* 2011; **13**: 1151–61. doi: <http://dx.doi.org/10.1093/neuonc/nor079>
  17. Oh J, Henry RG, Pirzkall A, Lu Y, Li X, Catalaa I, et al. Survival analysis in patients with glioblastoma multiforme: predictive value of choline-to-N-acetylaspartate index, apparent diffusion coefficient, and relative cerebral blood volume. *J Magn Reson Imaging* 2004; **19**: 546–54. doi: <http://dx.doi.org/10.1002/jmri.20039>
  18. Brandao LA, Domingues RC. Brain metabolites and their significance in spectral analysis. In: Brandao LA, Domingues RC, eds. *MR spectroscopy of the brain*. Philadelphia, PA: Lippincott Williams & Wilkins; 2004. pp. 11–12.
  19. Stel VS, Dekker FW, Tripepi G, Zoccali C, Jager KJ. Survival analysis I: the Kaplan-Meier method. *Nephron Clin Pract* 2011; **119**: c83–8. doi: <http://dx.doi.org/10.1159/000324758>
  20. Stel VS, Dekker FW, Tripepi G, Zoccali C, Jager KJ. Survival analysis II: Cox regression. *Nephron Clin Pract* 2011; **119**: c255–60. doi: <http://dx.doi.org/10.1159/000328916>
  21. Schoenfeld DA. Partial residuals for the proportional hazards regression model. *Biometrika* 1982; **39**: 499–503. doi: <http://dx.doi.org/10.2307/2531021>
  22. Shinojima N, Kochi M, Hamada J, Nakamura H, Yano S, Makino K, et al. The influence of sex and the presence of giant cells on postoperative long-term survival in adult patients with supratentorial glioblastoma multiforme. *J Neurosurg* 2004; **101**: 219–26. doi: <http://dx.doi.org/10.3171/jns.2004.101.2.0219>
  23. Salvati M, Cervoni L, Artico M, Caruso R, Gagliardi FM. Long-term survival in patients with supratentorial glioblastoma. *J Neurooncol* 1998; **36**: 61–4. doi: <http://dx.doi.org/10.1023/A:1017926603341>
  24. Romano A, Calabria LF, Tavanti F, Minniti G, Rossi-Espagnet MC, Coppola V, et al. Apparent diffusion coefficient obtained by magnetic resonance imaging as a prognostic marker in glioblastomas: correlation with MGMT promoter methylation status. *Eur Radiol* 2013; **23**: 513–20. doi: <http://dx.doi.org/10.1007/s00330-012-2601-4>
  25. Biomarkers Definitions Working Group. Biomarkers and surrogate endpoints: preferred definitions and conceptual framework. *Clin Pharmacol Ther* 2001; **69**: 89–95. doi: <http://dx.doi.org/10.1067/mcp.2001.113989>
  26. Kim H, Catana C, Ratai EM, Andronesi OC, Jennings DL, Batchelor TT, et al. Serial magnetic resonance spectroscopy reveals a direct metabolic effect of cediranib in glioblastoma. *Cancer Res* 2011; **71**: 3745–52. doi: <http://dx.doi.org/10.1158/0008-5472.CAN-10-2991>
  27. Law M, Yang S, Wang H, Babb JS, Johnson G, Cha S, et al. Glioma grading: sensitivity, specificity, and predictive values of perfusion MR imaging and proton MR spectroscopic imaging compared with conventional MR imaging. *AJNR Am J Neuroradiol* 2003; **24**: 1989–98.
  28. Leimgruber A, Ostermann S, Yeon EJ, Buff E, Maeder PP, Stupp R, et al. Perfusion and diffusion MRI of glioblastoma progression in a four-year prospective temozolomide clinical trial. *Int J Radiat Oncol Biol Phys* 2006; **64**: 869–75. doi: <http://dx.doi.org/10.1016/j.ijrobp.2005.08.015>
  29. Allen N. Oxidative metabolism of brain tumors. *Prog Exp Tumor Res* 1972; **17**: 192–209. doi: <http://dx.doi.org/10.1159/000393674>
  30. Zagzag D, Friedlander DR, Margolis B, Grumet M, Semenza GL, Zhong H, et al. Molecular events implicated in brain tumor angiogenesis and invasion. *Pediatr Neurosurg* 2000; **33**: 49–55. doi: <http://dx.doi.org/10.1159/000028975>
  31. Li Y, Lupo JM, Parvataneni R, Lamborn KR, Cha S, Chang SM, et al. Survival analysis in patients with newly diagnosed glioblastoma using pre- and postradiotherapy MR spectroscopic imaging. *Neuro Oncol* 2013; **15**: 607–17. doi: <http://dx.doi.org/10.1093/neuonc/nos334>
  32. Lim KS, Lim KJ, Price AC, Orr BA, Eberhart CG, Bar EE. Inhibition of monocarboxylate transporter-4 depletes stem-like glioblastoma cells and inhibits HIF transcriptional response in a lactate-independent manner. *Oncogene* 2014; **33**: 4433–41. doi: <http://dx.doi.org/10.1038/onc.2013.390>
  33. Jeremic B, Milicic B, Grujicic D, Dagovic A, Aleksandrovic J, Nikolic N. Clinical prognostic factors in patients with malignant glioma treated with combined modality approach. *Am J Clin Oncol* 2004; **27**: 195–204. doi: <http://dx.doi.org/10.1097/01.coc.0000055059.97106.15>

34. Teo M, Martin S, Owusu-Agyemang K, Nowicki S, Clark B, Mackinnon M, et al. A survival analysis of GBM patients in the West of Scotland pre- and post-introduction of the Stupp regime. *Br J Neurosurg* 2014; **28**: 351–5. doi: <http://dx.doi.org/10.3109/02688697.2013.847170>
35. Gorlia T, van den Bent MJ, Hegi ME, Mirimanoff RO, Weller M, Cairncross JG, et al. Nomograms for predicting survival of patients with newly diagnosed glioblastoma: prognostic factor analysis of EORTC and NCIC trial 26981-22981/CE.3. *Lancet Oncol* 2008; **9**: 29–38. doi: [http://dx.doi.org/10.1016/S1470-2045\(07\)70384-4](http://dx.doi.org/10.1016/S1470-2045(07)70384-4)
36. Lamborn KR, Chang SM, Prados MD. Prognostic factors for survival of patients with glioblastoma: recursive partitioning analysis. *Neuro Oncol* 2004; **6**: 227–35. doi: <http://dx.doi.org/10.1215/S1152851703000620>
37. Lacroix M, Abi-Said D, Fourney DR, Gokalan ZL, Shi W, DeMonte F, et al. A multivariate analysis of 416 patients with glioblastoma multiforme: prognosis, extent of resection, and survival. *J Neurosurg* 2001; **95**: 190–8. doi: <http://dx.doi.org/10.3171/jns.2001.95.2.0190>
38. Hattingen E, Bahr O, Rieger J, Blasel S, Steinbach J, Pilatus U. Phospholipid metabolites in recurrent glioblastoma: *in vivo* markers detect different tumor phenotypes before and under antiangiogenic therapy. *PLoS One* 2013; **8**: e56439. doi: <http://dx.doi.org/10.1371/journal.pone.0056439>